

# Validation of the Fokker-Planck Approach to Vibrational Kinetics in CO<sub>2</sub> Plasma

Pedro Viegas,<sup>\*,†</sup> Mauritius C. M. van de Sanden,<sup>†</sup> Savino Longo,<sup>‡</sup> and Paola  
Diomede<sup>\*,†</sup>

<sup>†</sup>*Center for Computational Energy Research, DIFFER - Dutch Institute for Fundamental  
Energy Research, De Zaale 20, 5612 AJ Eindhoven, The Netherlands*

<sup>‡</sup>*Dipartimento di Chimica, Università degli Studi di Bari, via Orabona 4, 70126 Bari, Italy*

E-mail: p.viegas@diffier.nl; p.diomede@diffier.nl

## Abstract

The Fokker-Planck (FP) approach to describe vibrational kinetics numerically is validated in this work. This approach is shown to be around 1000 times faster than the usual state-to-state (STS) method to calculate a vibrational distribution function (VDF) in stationary conditions. Weakly ionized, non-equilibrium CO<sub>2</sub> plasma is the test case for this demonstration, in view of its importance for the production of carbon-neutral fuels. VDFs obtained through the resolution of a FP equation and through the usual STS approach are compared in the same conditions and considering the same kinetic data. The demonstration is shown for chemical networks of increasing generality in vibrational kinetics of polyatomic molecules, including: V-V exchanges, V-T relaxation, intermode V-V' reactions and excitation through e-V collisions. The FP method is shown to be accurate to describe the vibrational kinetics of the CO<sub>2</sub> asymmetric stretching mode, while being much faster than the STS approach. In this way, the quantitative validity of the FP approach in vibrational kinetics is assessed,

making it a fully viable alternative to STS solvers, that can be used with other processes, molecules and physical conditions.

## Introduction

Vibrational kinetics has many applications in fields like catalysis, laser chemistry, atmospheric entry and plasma chemistry. In particular, in recent years much attention has been dedicated to low-temperature plasmas to convert greenhouse gas CO<sub>2</sub> into carbon-neutral fuels or useful chemicals<sup>1,2</sup>. Vibrational excitation of the CO<sub>2</sub> molecule, and in particular of its vibrational asymmetric stretching mode, is expected to play an important role in energy-efficient non-equilibrium dissociation kinetics<sup>3-6</sup>. The main tool used to model vibrational kinetics is the state-to-state (STS) finite rate method, based on the numerical solution of a master equation (ME)<sup>7-10</sup>. The ME is actually a stiff system of nonlinear ordinary differential equations (ODEs), as many as the number of states considered. When polyatomic molecules are involved, with a high number of vibrational levels and transitions, the computational efficiency of models describing reactors with spatial resolution and coupling different physical phenomena is compromised. Such models require new methods that allow a significant reduction in computational cost, while maintaining the accuracy on the description of vibrational kinetics. In recent years several methods have been developed that reduce the computational cost of models and aim at capturing the main features of vibrational kinetics in CO<sub>2</sub>. The work of Peerenboom *et al.*<sup>11</sup> has presented a dimension reduction method based on principal component analysis applied to a CO<sub>2</sub> plasma model. In the work of Berthelot and Bogaerts<sup>12</sup> a reduced CO<sub>2</sub> plasma chemistry set has been proposed, based on lumping the vibrational levels. Then, de la Fuente *et al.*<sup>13</sup> have presented a methodology for reduction of vibrational kinetics based on lumping the asymmetric vibrational levels of CO<sub>2</sub> into a single species, assuming a Treanor vibrational distribution and effective rate coefficients dependent on vibrational temperature. Moreover, in the paper by

Sahai *et al.*<sup>14</sup> a reduced-order model has been developed for N<sub>2</sub>, based on the coarse-grain maximum entropy method. Then, Kustova *et al.*<sup>15</sup> have developed multi-temperature models for CO<sub>2</sub>. Finally, in the work of Koelman *et al.*<sup>16</sup> pathway analysis has been proposed as a fast method to identify important mechanisms in CO<sub>2</sub> plasma chemistry. Although able to describe several features of plasma chemistry, none of these methods can fully depict the vibrational distribution function (VDF).

In the 1970s and 1980s, analytical theories have been developed that can describe the VDF taking into account different processes, without the STS method<sup>3,6,7,17-23</sup>. These are based on the continuous approximation, which transforms the ME for the VDF into a drift-diffusion Fokker-Planck (FP) equation. This approach is based on the idea of replacing the discrete internal levels by a continuum in the vibrational energy space, which allows to use concepts of transport theory to describe vibrational kinetics. In the works of the group of Rusanov and Fridman, analytical expressions have been presented for the fluxes in vibrational energy space, dependent on kinetic data. Firstly, in Rusanov *et al.*<sup>22</sup> the FP approach has been used to find analytically the VDF in diatomic molecules taking into account monoquantum vibrational energy losses to translation (V-T relaxation), vibrational energy exchanges (V-V relaxation) and losses of vibrationally excited states due to chemical reactions. Then, in another work by Rusanov *et al.*<sup>23</sup> monoquantum and multiquantum vibrational excitation of molecules by electron impact (e-V processes) and vibrational energy exchanges between various vibrational modes of the system (V-V' exchanges) have also been depicted over a single-mode energy space, which has allowed to apply the FP approach to the vibrational asymmetric stretching mode of polyatomic CO<sub>2</sub>. In Macheret *et al.*<sup>20</sup> the role of e-V processes in vibrational energy space has been described in more detail. In the books by Fridman<sup>3,19</sup>, the inclusion in the FP equation of monoquantum resonant V-V relaxation has also been described. Then, in the compilation by Capitelli (chapter 10)<sup>7</sup> and in the book by Fridman (chapter 5)<sup>19</sup>, all these processes have been described in polyatomic molecules over the total vibrational energy (sum of the vibrational energies of each mode) in the quasi-continuum

region, where intermode exchanges are expected to be very fast.

In recent publications by some of the authors of the present paper<sup>24-26</sup>, the FP approach has been implemented through numerical methods that avoid the approximations required in analytical solutions. In particular, in Diomedea *et al.*<sup>24</sup> the FP equation for the CO<sub>2</sub> asymmetric stretching vibrational mode has been solved numerically in time using a Monte Carlo technique based on the short-time Green function of the FP equation. Then, in Diomedea *et al.*<sup>25</sup> a much more effective method has been used, that solves the FP equation for the same system in stationary conditions in fractions of second. This method consists on matching the VDF with the V-V dissociation rate of CO<sub>2</sub>, and thus with the flux of the CO<sub>2</sub> population in energy space. In this work, the flux-matching method presented in Diomedea *et al.*<sup>25</sup> is used to solve the FP equation for the CO<sub>2</sub> asymmetric stretching vibrational mode. The method and parameters used within are validated by comparing the resulting VDFs with those obtained through a STS model considering the same physical conditions and kinetic data. First, the derivation of the FP equation is presented, along with its theoretical limits of validity. Then, the numerical methods to solve both the STS and FP models are presented, along with the parameters considered. Finally, the parameters used to describe each chemical process in the FP model are validated by comparing STS and FP VDFs resulting from each process separately.

## Methods

### a. Derivation of the Fokker-Planck equation

The derivation of the Fokker-Planck equation to describe population kinetics is found in the compilation by Lifshitz and Pitaevskii (chapter II)<sup>27</sup>, in the book by van Kampen (chapter VIII)<sup>28</sup> and in the book by Biberman *et al.* (chapter 5.4 and appendix 2)<sup>29</sup> and is briefly exposed in this section. The population density at time  $t$  of each state  $k$  in a molecule,  $n_k$ ,

is determined from the gain-loss balance equation:

$$\frac{dn_k}{dt} = \sum_j [n_j \omega_{jk} - n_k \omega_{kj}] \quad (1)$$

where  $\omega_{jk}$  is the probability of a transition from state  $j$  to state  $k$  per unit time.

In the energy space of the vibrational asymmetric stretching mode of CO<sub>2</sub>, the maximum internal energy  $\epsilon_{max}$  is the dissociation energy 5.467 eV, calculated as in Kozák and Bogaerts<sup>30</sup>. The discrete vibrational states within are distanced in energy by less than 0.3 eV, much less than  $\epsilon_{max}$ . Thus, the states are close in the space of vibrational energy and we can assume they form a continuum in energy space. By changing variables to the population density per energy  $f(\epsilon) = n_k dk/d\epsilon$  (units cm<sup>-3</sup>eV<sup>-1</sup>) and to the transition probability per energy  $w(\epsilon, \epsilon') = \omega_{kj} dk/d\epsilon$  (units eV<sup>-1</sup>s<sup>-1</sup>), we can rewrite eq. 1 as function of the energy  $\epsilon$  of state  $k$  and the energies  $\epsilon'$  of states  $j$ :

$$\frac{df(\epsilon)}{dt} = \int [f(\epsilon')w(\epsilon', \epsilon) - f(\epsilon)w(\epsilon, \epsilon')]d\epsilon' = \quad (2)$$

$$= \int f(\epsilon - r)w(\epsilon - r; r)dr - \int f(\epsilon)w(\epsilon; -r)dr \quad (3)$$

where  $r = \epsilon - \epsilon'$  is the jump in energy in each transition  $w(\epsilon'; r)$  from energy  $\epsilon'$  to  $\epsilon$ . Then, we take an assumption that only small energy jumps take place:  $r \ll \epsilon_{max}$ . Monoquantum transitions in the energy space of the vibrational asymmetric stretching mode require a jump always inferior to 0.3 eV. Thus, we consider that the assumption of small jumps is valid in a system where only these monoquantum transitions take place. The first integral in eq. 3 can then be expanded in a Taylor series:

$$\frac{df(\epsilon)}{dt} = \int f(\epsilon)w(\epsilon; r)dr + \sum_{m=1}^{\infty} \frac{(-1)^m}{m!} \frac{d^m}{d\epsilon^m} [a_m(\epsilon)f(\epsilon)] - \int f(\epsilon)w(\epsilon; -r)dr \quad (4)$$

$$a_m(\epsilon) = \int r^m w(\epsilon; r)dr \quad (5)$$

where we call  $a_m$  the jump moments of order  $m$ . Under the assumption of small jumps and of detailed balance, the transition probabilities  $w(\epsilon; r)$  and  $w(\epsilon; -r)$  are equal and the first and last terms in eq. 4 cancel each other. Then, by truncating the Taylor expansion at the second term, we obtain the Fokker-Planck equation:

$$\frac{df(\epsilon)}{dt} = -\frac{d}{d\epsilon}[a_1(\epsilon)f(\epsilon)] + \frac{1}{2}\frac{d^2}{d\epsilon^2}[a_2(\epsilon)f(\epsilon)] = -\frac{dJ(\epsilon)}{d\epsilon} \quad (6)$$

$$J(\epsilon) = A(\epsilon)f(\epsilon) - B(\epsilon)\frac{df(\epsilon)}{d\epsilon} \quad (7)$$

$$A(\epsilon) = a_1(\epsilon) - \frac{1}{2}\frac{da_2(\epsilon)}{d\epsilon}; B(\epsilon) = \frac{1}{2}a_2(\epsilon) \quad (8)$$

where  $J$  is the flux of population  $f(\epsilon)$  in energy space (units  $\text{cm}^{-3}\text{s}^{-1}$ ) through drift and diffusion processes,  $A$  is the drift coefficient and  $B$  the diffusion coefficient. As a result, we use eq. 6 to describe the population of  $\text{CO}_2$  molecules in the energy space of the vibrational asymmetric stretching mode, considering that only monoquantum transitions are relevant. We calculate the jump moments in eq. 5 by summing the contributions of all the processes  $p$  considered:

$$a_m(\epsilon) = \sum_p [r(\epsilon)]^m k_p(\epsilon) n_p \quad (9)$$

where  $k_p$  is the rate coefficient of process  $p$  and  $n_p$  is the number density of the collision partner of  $\text{CO}_2$  with energy  $\epsilon$  in process  $p$ . The processes considered and their implementation are described in the next sections.

## b. State-to-state model

In order to validate the implementation and use of the Fokker-Plank (FP) equation for the system under study, we compare its results with those from a state-to-state (STS) model that solves the rate balance equations for discrete states (eq. 1), considering the exact same processes and kinetic data as the FP model. The STS model is based on the scheme in the paper of Kozák and Bogaerts<sup>30</sup>, focusing on the vibrational kinetics of the asymmet-

ric stretching mode of CO<sub>2</sub>, the one with more influence on the dissociation rates. Other reaction schemes provide a more complete description of the coupling between vibrational modes<sup>9,10,31</sup>. In this validation exercise, the specificities of the reaction scheme are not the main concern and we chose the kinetics in Kozák and Bogaerts<sup>30</sup> for benchmarking purposes, as in our previous works. The STS model used in this work is simplified with respect to the one in Kozák and Bogaerts<sup>30</sup>, assuming low dissociation of CO<sub>2</sub>, to address directly the validation of the FP approach. The low dissociation assumption allows to neglect the role of reactions involving other species on the VDF.

A total of 30 species is considered: electrons, positive ion CO<sub>2</sub><sup>+</sup>, the products of dissociation CO and O, ground-state CO<sub>2</sub>, the vibrationally-excited states of CO<sub>2</sub> purely in the symmetric stretching and bending modes CO<sub>2</sub>( $v_a, v_b, v_c, v_d$ ) and the vibrationally-excited states of CO<sub>2</sub> purely in the asymmetric stretching mode CO<sub>2</sub>( $v = 1 - 21$ ). We take the definition and vibrational energy of the CO<sub>2</sub> states as in the paper by Kozák and Bogaerts<sup>30</sup>, taking the ground-state as reference with zero energy. The processes listed in table 1 are considered, with rate coefficients taken from Kozák and Bogaerts<sup>30</sup>. Keeping consistency with the derivation in the previous section, we consider monoquantum exchange processes are the most relevant for the asymmetric stretching mode and thus are the only ones taken into account. Besides ionization, electron recombination and electron-impact vibrational excitation, intramode monoquantum vibration-vibration (V-V) exchanges in the asymmetric stretching mode are considered. We take collisions with the most populated states CO<sub>2</sub>( $v = 1$ ) (forward reactions) and CO<sub>2</sub>( $v = 0$ ) (reverse reactions), called V-V<sub>1</sub>, as well as quasi-resonant collisions between states with the same energy and corresponding reverse reactions, called V-V<sub>*n*</sub>, that introduce increasing non-linearity in the system. Moreover, monoquantum vibration-translation (V-T) exchanges are considered purely in the asymmetric stretching mode (CO<sub>2</sub>( $v = 0 - 21$ )) and in the joint symmetric stretching and bending modes (CO<sub>2</sub>( $v = 0, v_a, v_b, v_c, v_d$ )), as in Kozák and Bogaerts<sup>30</sup>. Then, intermode vibration-vibration (V-V') transitions are considered as collisions of molecules excited in the

asymmetric stretching mode with those in highly populated states: ground state and excited in the bending and symmetric stretching modes  $\text{CO}_2(v_a, v_b)$ , as in Kozák and Bogaerts<sup>30</sup>. Dissociation is taken into account through the monoquantum V-V<sub>1</sub> and V-V<sub>n</sub> forward mechanisms. Rate coefficients for V-V dissociation processes are obtained from fits of the rate coefficients of V-V processes as function of the vibrational energy, evaluated at the dissociation energy 5.467 eV, as in our previous works<sup>24,25</sup>. Finally, three-body recombination of CO and O into ground-state  $\text{CO}_2$  is considered, as in Kozák and Bogaerts<sup>30</sup>, thus closing the system.

Table 1: List of processes in the STS model. M represents any neutral species.

Process name	Reaction
Ionization	$e + \text{CO}_2(v = 0) \rightarrow \text{CO}_2^+ + 2 e$
e-recomb.	$e + \text{CO}_2^+ \rightarrow \text{CO}_2(v = 0) (\text{CO} + \text{O}, \text{C} + \text{O}_2)$
e-V	$e + \text{CO}_2(v = n) \leftrightarrow e + \text{CO}_2(v = n + 1), n = 0 - 5$
V-V <sub>1</sub>	$\text{CO}_2(v = n) + \text{CO}_2(v = 1) \leftrightarrow \text{CO}_2(v = n + 1) + \text{CO}_2(v = 0), n = 1 - 20$
V-V <sub>n</sub>	$\text{CO}_2(v = n) + \text{CO}_2(v = n) \leftrightarrow \text{CO}_2(v = n + 1) + \text{CO}_2(v = n - 1), n = 1 - 20$
V - T	$\text{CO}_2(v = n) + \text{M} \leftrightarrow \text{CO}_2(v = n - 1) + \text{M}, n = 1 - 21$ $\text{CO}_2(v_a, v_b, v_c, v_d) + \text{M} \leftrightarrow \text{CO}_2(v = 0, v_a, v_b, v_c) + \text{M}$
V-V' <sub>a</sub>	$\text{CO}_2(v = n) + \text{CO}_2(v = 0) \leftrightarrow \text{CO}_2(v = n - 1) + \text{CO}_2(v_a), n = 1 - 21$
V-V' <sub>b</sub>	$\text{CO}_2(v = n) + \text{CO}_2(v = 0) \leftrightarrow \text{CO}_2(v = n - 1) + \text{CO}_2(v_b), n = 1 - 21$
V-V <sub>1</sub> diss.	$\text{CO}_2(v = 21) + \text{CO}_2(v = 1) \rightarrow \text{CO} + \text{O} + \text{CO}_2(v = 0)$
V-V <sub>n</sub> diss.	$\text{CO}_2(v = 21) + \text{CO}_2(v = 21) \rightarrow \text{CO} + \text{O} + \text{CO}_2(v = 20)$
$\text{CO}_2$ recomb.	$\text{CO} + \text{O} + \text{M} \rightarrow \text{CO}_2(v = 0) + \text{M}$

We consider a relatively high pressure  $p = 100$  mbar, fixed gas temperature  $T_g = 300$  K and gas density  $n_g = 2.414 \times 10^{18} \text{ cm}^{-3}$ . We assume a constant input power density  $P_{dep}$  transferred to the electrons and thus the temporal evolution of the electron mean energy  $\epsilon_m$  is described by the electron energy equation:

$$\frac{d(n_e \epsilon_m)}{dt} = P_{dep}(t) - \frac{P_{el}}{n_g}(\epsilon_m) n_g n_e - \frac{P_{inel}}{n_g}(\epsilon_m) n_g n_e \quad (10)$$

where  $n_e$  is the electron number density and  $P_{el}$  and  $P_{inel}$  are the components of the power lost by electrons through elastic and inelastic collisions, respectively. The electron-impact rate coefficients and the electron power losses are obtained as function of  $\epsilon_m$  from the solution

of the electron Boltzmann equation solver BOLSIG+<sup>32</sup>, using the electron-impact cross sections from the Phelps database in LXCat<sup>33,34</sup>, as has been done in the work of Kozák and Bogaerts<sup>30</sup>. The set of ODEs is solved until reaching a stationary condition with the solver RADAU5, an implicit Runge-Kutta method of order 5<sup>35,36</sup>. This solver has been used in other zero-dimensional plasma chemistry models<sup>37,38</sup>. We take as initial conditions  $n_e = [\text{CO}_2^+] = 7.5 \times 10^{10} \text{ cm}^{-3}$  and  $\epsilon_m = 1.0 \text{ eV}$ . The criterion for stationary condition is  $\max(|\frac{n_i(t)-n_i(t-\Delta t)}{n_i(t-\Delta t)}|) < 10^{-8}$ , where  $i$  is the index for each of the species considered.

Using this model, the electron energy and rate equations are solved to provide the stationary  $n_e$  and  $\epsilon_m$  as function of the input  $P_{dep}$ . Together with the other rate equations, they also provide  $T_{va}$ , the vibrational temperature of the asymmetric stretching vibrational mode, and  $T_{vs}$ , the vibrational temperature of the bending, together with symmetric stretching, vibrational modes. These temperatures are input parameters for the FP model and thus are necessary for the validation procedure.  $T_{va}$  and  $T_{vs}$  are calculated from the densities of states  $\text{CO}_2(v=0)$ ,  $\text{CO}_2(v=1)$  and  $\text{CO}_2(v_a)$ , considering Boltzmann distributions. Moreover, the VDF for the asymmetric stretching vibrational mode is obtained in the STS model, essentially defined by the V-V, V-T, V-V' and e-V processes in table 1. The computational time on a single CPU for a STS calculation to reach a stationary condition is typically between 1 and 10 minutes.

### c. Fokker-Planck flux-matching model

The computational method to solve the FP eq. 6 is the same as in Diomede *et al.*<sup>25</sup>. We solve the FP equation only for a stationary condition, when  $df/dt = -dJ/d\epsilon = 0$ . As the flux  $J$  is uniform in energy space, we can consider it as a fixed parameter. By dividing eq. 7 by  $B(\epsilon)f(\epsilon)$ , we obtain:

$$\frac{d \ln[f(\epsilon)]}{d \epsilon} = \frac{A(\epsilon)}{B(\epsilon)} - \frac{J}{B(\epsilon)f(\epsilon)} \quad (11)$$

This equation can be solved immediately by forward numerical integration, although  $f(\epsilon)$

appears in the right-hand side.  $A(\epsilon)$  and  $B(\epsilon)$  are the only required input parameters. These are calculated as described in eqs. 8 and 9 and are dependent on temperatures and densities known from the STS results. Their calculation for each process will be described in the next sections. As in the previous works<sup>24,25</sup>, for each process, the coefficients  $k(\epsilon)$  used in the calculation of  $A(\epsilon)$  and  $B(\epsilon)$  are fit to the discrete kinetic data from Kozák and Bogaerts<sup>30</sup> at  $T_g = 300$  K. The VDF (units  $\text{cm}^{-3}$ )  $n(\epsilon)$  is obtained from the population density per energy  $f(\epsilon)$  as follows:

$$n(\epsilon) = \int f(\epsilon') \delta(\epsilon' - \epsilon) d\epsilon' \quad (12)$$

where  $\delta$  is the Kronecker delta. The left boundary condition is  $n(0) = n_0$ , density of the ground-state, known from the STS results. Then, as  $J$  is uniform, it is equal to its value at the dissociation energy 5.467 eV. That is the dissociation flux, exclusively by V-V monoquantum reactions V-V<sub>1</sub> and V-V<sub>*n*</sub>, equal to the STS dissociation rate:

$$J_{diss} = n(\epsilon_{max})[k_{VV1}(\epsilon_{max})n_1 + k_{VVn}(\epsilon_{max})n(\epsilon_{max})] \quad (13)$$

where  $n_1$  is obtained from the STS results and  $n(\epsilon_{max})$  is self-consistently obtained through eq. 12. In more complex chemical networks, dissociation can occur from states of lower energy than the uppermost bound one and through several processes. For such cases, the right-hand side of eq. 13 is an integral operator acting on  $n(\epsilon)$  and the dissociation rates  $k(\epsilon)$ .

Equations 11 and 13 form a functional problem that is solved in the energy grid between the energy of the ground-state and the dissociation energy, from 0 to 5.467 eV. An initial  $J = 0$  is assumed to solve eq. 11, then a new  $J_{diss}$  is calculated from eq. 13, then a new  $J$  is guessed through a binary search algorithm. The process is repeated iteratively until the guessed  $J$  converges with the calculated  $J_{diss}$ . Then, the flux and the VDF are matched. The convergence criterion has been set as  $10^{-6}$  and it typically takes around 25 iterations to reach it. The energy grid has been divided in 5,000 bins of approximately 0.001 eV length.

The computational time of the FP simulation on the same single CPU is typically three orders of magnitude lower than the one of the STS calculations, around 0.1 seconds.

## Results: Validation of the Fokker-Planck approach

### a. V-V<sub>1</sub> processes only

V-V<sub>1</sub> processes are exchanges where CO<sub>2</sub> molecules gain a vibrational quantum by colliding with molecules excited at level  $v = 1$ , the most populated excited state in the vibrational asymmetric stretching mode, that lose a quantum in the collision. These reactions are expected to define the bulk of the VDF of the asymmetric stretching vibrational mode of CO<sub>2</sub>. If a VDF is exclusively defined by these reactions, and no dissociation takes place, which is a non-physical condition, a Treanor VDF is expected<sup>39</sup> (eq. 3.7 in that paper):

$$n(v) = n_0 \exp \left[ -\frac{v E_1}{T_{va}} + \frac{v E_1 - E_v}{T_g} \right] \quad (14)$$

where  $E_v$  is the internal energy of level  $v$ .

To test this hypothesis, we perform STS calculations only with ionization, electron-ion recombination, e-V (between CO<sub>2</sub>( $v = 0$ ) and CO<sub>2</sub>( $v = 1$ ) only) and V-V<sub>1</sub> (without dissociation) processes listed in table 1 and with  $P_{dep} = 50 \text{ W cm}^{-3}$ . The resulting VDF has  $T_{va} = 2422 \text{ K}$ , which represents a very high vibrational non-equilibrium, considering that  $T_g = 300 \text{ K}$ . The VDF is presented in Fig. 1, where it is shown to fit the theoretical Treanor VDF of eq. 14. Then, with the FP model, we solve eq. 11 imposing  $J = 0$ . In this situation, the stationary VDF is not determined by the values of the transport coefficients  $A$  and  $B$ , but only by the ratio between them. As we assume that the VDF is Treanor, we can define  $A$  as function of  $B$  from eq. 11 together with the continuum approximation of the Treanor VDF as follows:

$$A_{VV1}(\epsilon) = B_{VV1}(\epsilon) \left[ -\frac{1}{T_g} + E_1 \frac{dv}{d\epsilon} \left( \frac{1}{T_g} - \frac{1}{T_{va}} \right) \right] \quad (15)$$

where  $dv/d\epsilon$  for  $\epsilon$  between  $E_{v-1}$  and  $E_v$  is defined as  $1/(E_v - E_{v-1})$ . Then, the only input required to solve the FP equation is  $T_{va}$ , obtained from the STS calculations. It can be verified in Fig. 1 that the resulting VDF matches the Treanor VDF and the STS result. This result establishes the relation between  $A_{VV_1}(\epsilon)$  and  $B_{VV_1}(\epsilon)$  in the Fokker-Planck model. In the work of Rusanov *et al.*<sup>22</sup> a similar reasoning is taken to define the flux due to V-V processes, but a formulation of the Treanor VDF is used that is slightly different than the one in Treanor's original paper<sup>39</sup>.

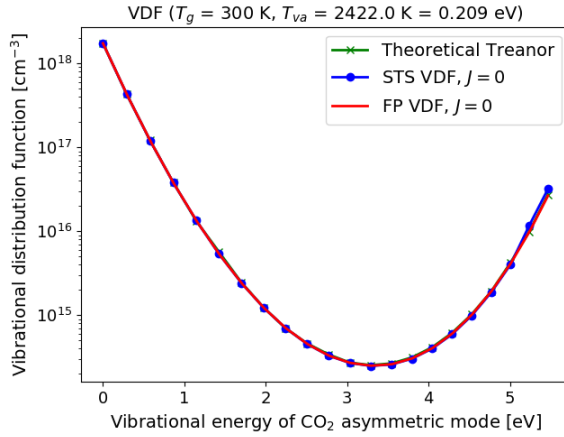


Figure 1: VDFs obtained exclusively with V-V<sub>1</sub> processes and without dissociation, for  $P_{dep} = 50 \text{ W cm}^{-3}$ . Results from STS model, FP model and Treanor VDF from theory in eq. 14.

If we remove the non-physical condition of no V-V<sub>1</sub> dissociation, the flux  $J$  in eq. 11 can no longer be ignored. Then, the solution of the stationary VDF depends not only on the ratio between  $A$  and  $B$  but also on their values. Following eqs. 8 and 9, and considering both forward and reverse V-V<sub>1</sub> exchanges, we have first tried to write the diffusion coefficient for V-V<sub>1</sub> processes as:

$$B_{VV_1}(\epsilon) = \frac{1}{2}[\Delta E(\epsilon)]^2[k_{VV_1f}(\epsilon)n_1 + k_{VV_1r}(\epsilon)n_0] \quad (16)$$

where  $\Delta E(\epsilon)$  for  $\epsilon$  between  $E_{v-1}$  and  $E_v$  is defined as  $E_v - E_{v-1}$ ,  $k_{VV_1f}$  is the rate coefficient of the forward process and  $k_{VV_1r}$  is the rate coefficient of the reverse process. Using the formulation in eq. 16, the agreement with the STS VDF is not satisfactory for energies

above 5 eV. An alternative formulation consists on considering forward and reverse V-V<sub>1</sub> processes together, with rate coefficient  $k_{VV_1}(\epsilon) = k_{VV_1f}(\epsilon) + k_{VV_1r}(\epsilon)$ . In this case, the density of the collision partner consists also of the sum of the densities of the collision partners of the forward and reverse processes. Thus, the diffusion coefficient is written as:

$$B_{VV_1}(\epsilon) = \frac{1}{2}[\Delta E(\epsilon)]^2 k_{VV_1}(\epsilon)[n_1 + n_0] \quad (17)$$

This is the approach used also for the description of the other processes impacting the VDF with forward and reverse reactions.  $A_{VV_1}(\epsilon)$  is calculated as in eq. 15. The resulting VDF, along with the dissociation rate  $J$ , is shown in Fig. 2 to match the STS result with  $T_{va} = 2074$  K, which validates the approach taken.  $J$  is only due to monoquantum V-V<sub>1</sub> processes, which is not expected to be a relevant dissociation mechanism, and thus should not be compared to the total dissociation taking place under experimental conditions.

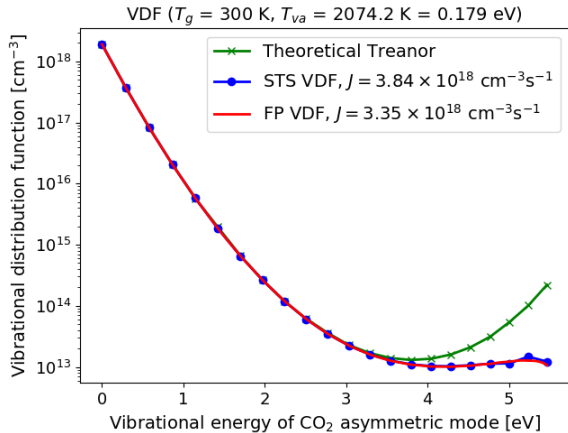


Figure 2: VDFs obtained exclusively with V-V<sub>1</sub> processes, including dissociation, for  $P_{dep} = 50$  W cm<sup>-3</sup>. Results from STS model, FP model and Treanor VDF from theory in eq. 14.

By comparing Figs. 1 and 2, it is visible that dissociation deviates the tail of the VDF from the Treanor VDF for energies above 3.5 eV, while the bulk of the VDF still follows the Treanor distribution. This result confirms that the Treanor VDF is only valid up to its minimum, as noticed in our previous works<sup>24-26</sup> and in the original paper by Treanor *et al.*<sup>39</sup>. Afterwards, a plateau of the VDF extends almost to the dissociation threshold. Moreover,

the inclusion of V-V<sub>1</sub> dissociation decreases  $T_{va}$  by about 348 K.

## b. V-T relaxation

V-T processes are exchanges between vibrational energy and translational energy, or heating, of gas molecules. When all the V-T processes listed in table 1 are included in the numerical models, without any other process, a Boltzmann VDF at gas temperature  $T_g$  is obtained in stationary condition. Following the same reasoning as for the V-V<sub>1</sub> processes, we can define  $A$  as function of  $B$  from eq. 11 together with the definition of the Boltzmann VDF as follows:

$$A_{VT}(\epsilon) = B_{VT}(\epsilon) \left[ -\frac{1}{T_g} \right] \quad (18)$$

Then, following eqs. 8 and 9, along with the description of the V-V<sub>1</sub> processes in the previous section, we write the diffusion coefficient as:

$$B_{VT}(\epsilon) = \frac{1}{2} [\Delta E(\epsilon)]^2 k_{VT}(\epsilon) [n_M + n_M] \quad (19)$$

where  $n_M$  is the density of any neutral species. When the V-V<sub>1</sub> and V-T processes are combined, with the same  $P_{dep} = 50 \text{ W cm}^{-3}$ , the obtained  $T_{va}$  is 714 K and the calculated VDF approaches a Boltzmann distribution. The inclusion of the V-T processes severely decreases  $T_{va}$ , mostly due to V-T reactions acting on the lowest states. Then, with  $P_{dep} = 2,000 \text{ W cm}^{-3}$ , 40 times higher than  $P_{dep}$  in the previous cases, the STS and FP VDFs shown in Fig. 3, together with the correspondent dissociation rates, are obtained with  $T_{va} = 1775 \text{ K}$ . Fig. 3 shows an excellent agreement between the STS and FP results. Even though V-T reactions decrease  $T_{va}$ , they do not deviate the tail of the VDF from the Treanor distribution any more than the V-V<sub>1</sub> dissociation studied in Fig. 2. This is due to the polyatomic character of CO<sub>2</sub>, that renders intermode V-V' exchanges very important at high internal energies and diminishes the role of V-T relaxation at those energies. This diminished role of V-T exchanges in the asymmetric stretching mode has been highlighted before in the work

of Armenise and Kustova<sup>9</sup>.

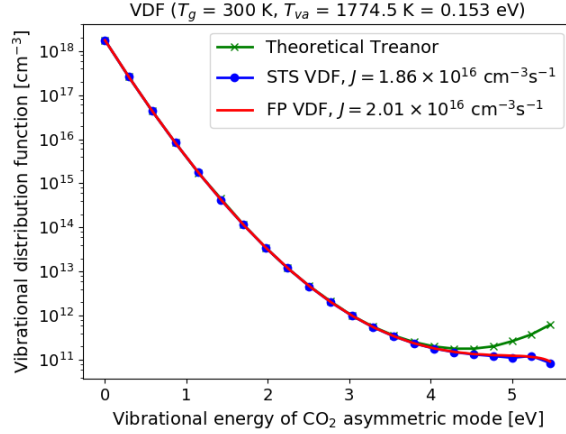


Figure 3: VDFs obtained with V-T and V-V<sub>1</sub> processes, including dissociation, for  $P_{dep} = 2000 \text{ W cm}^{-3}$ . Results from STS model, FP model and Treanor VDF from theory in eq. 14.

### c. V-V' exchange

V-V' processes are exchanges of vibrational energy between the different vibrational modes of CO<sub>2</sub>. Instead of leading the VDF towards a Treanor distribution at the vibrational temperature of the asymmetric stretching mode, V-V' processes between two modes contribute to a Treanor distribution of a two-mode oscillator<sup>6,23</sup>. Thus, the relation between  $A$  and  $B$  for V-V' processes between the asymmetric mode ( $a$ ) and the combination of the symmetric stretching and bending modes ( $s$ ) is written as:

$$A_{VV'}(\epsilon) = B_{VV'}(\epsilon) \left[ -\frac{1}{T_g} + E_1 \frac{dv}{d\epsilon} \left( \frac{1}{T_g} - \beta_{as} \right) \right] \quad (20)$$

$$\beta_{as} = \frac{\omega_s}{\omega_a T_{vs}} + \frac{\omega_a - \omega_s}{\omega_a T_g} \quad (21)$$

where  $\omega_a$  is the vibrational frequency of the asymmetric stretching mode and  $\omega_s$  is the vibrational frequency of the symmetric stretching mode, the highest between the vibrational frequencies of the symmetric stretching and bending modes. This collisional data is obtained from Kozák and Bogaerts<sup>30</sup>. Then, following eqs. 8 and 9, we write the diffusion coefficient

as:

$$B_{VV'_a}(\epsilon) = \frac{1}{2}[\Delta E(\epsilon)]^2 k_{VV'_a}(\epsilon)[n_0 + n_a] \quad (22)$$

$$B_{VV'_b}(\epsilon) = \frac{1}{2}[\Delta E(\epsilon)]^2 k_{VV'_b}(\epsilon)[n_0 + n_b] \quad (23)$$

$$B_{VV'}(\epsilon) = B_{VV'_a}(\epsilon) + B_{VV'_b}(\epsilon) \quad (24)$$

where  $n_a$  and  $n_b$  are respectively the densities of states  $\text{CO}_2(v_a)$  and  $\text{CO}_2(v_b)$ , vibrationally excited in the bending and symmetric stretching modes, obtained from the STS results. When the V-V' processes are combined with the V-V<sub>1</sub> and V-T processes, at the same  $P_{dep} = 2000 \text{ W cm}^{-3}$ ,  $T_{va}$  is 1333 K, around 442 K lower than in the case without V-V' processes. V-V' processes, along with V-T relaxation, are thus important for the calculation of  $T_{va}$ . Then, with  $P_{dep} = 20,000 \text{ W cm}^{-3}$ , 10 times higher than  $P_{dep}$  in the previous case without V-V' processes, the STS and FP VDFs shown in Fig. 4 are obtained with  $T_{va} = 2505 \text{ K}$ . An excellent agreement is obtained between the STS and FP VDFs. Moreover, we notice in Fig. 4 a serious deviation of the tail of the VDF from the Treanor distribution, for  $\epsilon > 3 \text{ eV}$ . Due to this deviation, the dissociation rate  $J$  presented in Fig. 4 is two orders of magnitude lower than  $J$  in Fig. 3 and four orders of magnitude lower than  $J$  in Fig. 2, despite the higher  $T_{va}$  of 2505 K in Fig. 4. This deviation is not obtained with other processes, which reinforces the relevance of V-V' exchanges. The importance of intermode exchanges has been highlighted before in the work of Armenise and Kustova<sup>31</sup>. With V-V<sub>1</sub>, V-T and V-V' processes, using the kinetic data from Kozák and Bogaerts<sup>30</sup>, we see that a rather complete description of the VDF can be depicted.

In Fig. 5 the agreement between STS and FP VDFs is evaluated for further conditions of  $P_{dep}$ , between 2,000 and 50,000  $\text{W cm}^{-3}$ . Consequently, a wide range of relevant values of  $T_{va}$  is assessed, between 1333 and 2831 K. We notice in every case a good agreement between the STS and FP VDFs. In fact, the distribution is the same until approximately 4 eV. Then, a small deviation of the tail of the FP VDF with respect to the STS VDF is visible for  $T_{va} =$

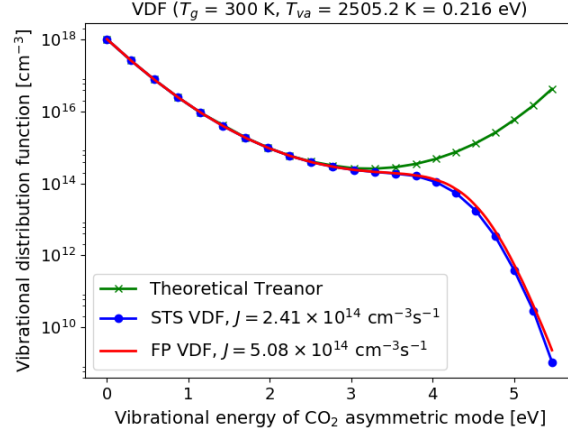


Figure 4: VDFs obtained with V-V', V-T and V-V<sub>1</sub> processes, including dissociation, for  $P_{dep} = 20,000 \text{ W cm}^{-3}$ . Results from STS model, FP model and Treanor VDF from theory in eq. 14.

1333 and 2831 K. This small deviation reflects the uncertainty in the approximations and parameters considered in the derivation of transport coefficients described so far, particularly when considering that V-V' processes are described by a Treanor distribution for a two-mode oscillator. As far as  $J$  is concerned, it is directly proportional to  $n_1$  and  $n(\epsilon_{max})$ , and thus the difference between STS and FP results of  $J$  is proportional to the difference between STS and FP results of  $n(\epsilon_{max})$ .

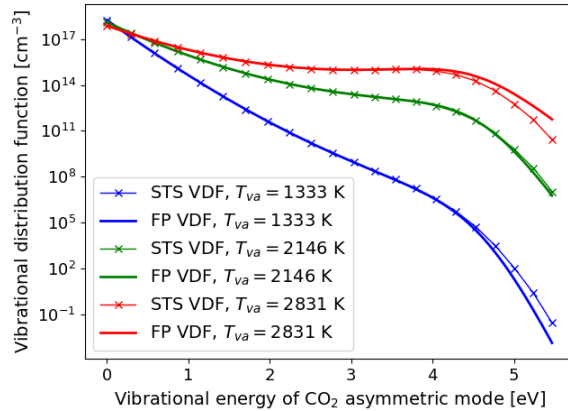


Figure 5: VDFs obtained with V-V', V-T and V-V<sub>1</sub> processes, including dissociation, for  $P_{dep} = 2,000; 10,000$  and  $50,000 \text{ W cm}^{-3}$ . Results from STS and FP models.

### d. V-V<sub>n</sub> processes

V-V<sub>n</sub> processes are exchanges where CO<sub>2</sub> molecules gain a vibrational quantum in the asymmetric stretching mode by colliding with molecules excited at the same level  $v = n$  that lose a quantum in the same mode in the collision. Therefore, the V-V<sub>n</sub> flux is nonlinear with respect to the VDF. An analytical expression for this flux is provided in Fridman's books<sup>3,19</sup>, which is different than the one used for other V-V processes, such as V-V<sub>1</sub>. In fact, following the formulation proposed in those works, the Treanor distribution is one solution to the VDF exclusively with V-V<sub>n</sub> processes and without dissociation ( $J = 0$ ), but is not the only solution, contrarily to other V-V processes. Instead of applying the rather complex analytical formulation proposed in Fridman's books<sup>3,19</sup>, we describe the relation between  $A$  and  $B$  for V-V<sub>n</sub> processes the same way we do for non-resonant V-V<sub>1</sub> processes in eq. 15. Then, we define the diffusion coefficient:

$$B_{VV_n}(\epsilon) = \frac{1}{2}[\Delta E(\epsilon)]^2 k_{VV_n}(\epsilon)[n(\epsilon) + n(\epsilon)] \quad (25)$$

The validity of this solution is tested by comparing the STS and FP VDFs for the same  $P_{dep}$  as in Fig. 5, now including V-V<sub>n</sub> processes. The results of this comparison are presented in Fig. 6.

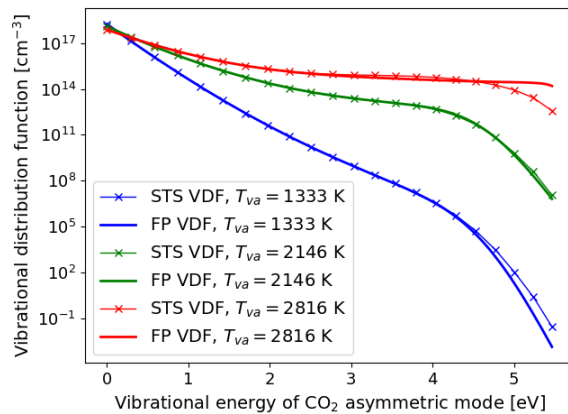


Figure 6: VDFs obtained with V-V<sub>n</sub>, V-V', V-T and V-V<sub>1</sub> processes, including dissociation, for  $P_{dep} = 2, 000; 10, 000$  and  $50, 000 \text{ W cm}^{-3}$ . Results from STS and FP models.

Firstly, it can be observed in Fig. 6 that  $T_{va}$  calculated through the STS simulations for the two cases of lower  $P_{dep}$  is the same as in Fig. 5. In the remaining case, with  $P_{dep} = 50,000 \text{ W cm}^{-3}$ ,  $T_{va}$  is slightly lower when including V-V<sub>n</sub> processes. Indeed, we verify that for  $T_g = 300 \text{ K}$  and  $T_{va} < 2500 \text{ K}$ , as the densities of the highest levels are relatively low, V-V<sub>n</sub> processes can be considered irrelevant and the V-V dissociation rate is almost exclusively due to V-V<sub>1</sub> processes. Thus, in that condition the agreement between the STS and FP VDFs is equally good, with or without the inclusion of V-V<sub>n</sub> collisions.

For  $T_{va} > 2500 \text{ K}$ , the relevance of V-V<sub>n</sub> processes increases with  $T_{va}$  and affects mostly the tail of the VDF and thus the V-V dissociation rate. With  $T_{va}$  around 2800 K, the dissociation rate in the STS results without V-V<sub>n</sub> processes in Fig. 5 is  $4.99 \times 10^{15} \text{ cm}^{-3} \text{ s}^{-1}$ , while with V-V<sub>n</sub> reactions in Fig. 6 it increases to  $1.31 \times 10^{18} \text{ cm}^{-3} \text{ s}^{-1}$ . Then, by comparing the STS and FP VDFs in Fig. 6 for the same  $T_{va}$ , we observe an agreement until approximately  $\epsilon = 3 \text{ eV}$ . However, the tail of the VDF calculated through the FP approach is significantly higher than the one of the STS VDF, which has an impact on  $J$ . When including V-V<sub>n</sub> reactions, the V-V<sub>1</sub> dissociation rate alone is much higher than in the STS results, due to the increase of the VDF tail:  $J_{diss-1} = 2.89 \times 10^{19} \text{ cm}^{-3} \text{ s}^{-1}$ . Moreover, the V-V<sub>n</sub> dissociation rate in those conditions is even higher:  $J_{diss-n} = 1.07 \times 10^{21} \text{ cm}^{-3} \text{ s}^{-1}$ . We conclude that our approach to include V-V<sub>n</sub> processes in the FP model can be used to describe the bulk of the VDF but not the tail for  $T_{va} > 2500 \text{ K}$  and  $T_g = 300 \text{ K}$ . We should notice that  $T_{va}/T_g \simeq 8$  represents an extremely high vibrational nonequilibrium, hardly reachable in experimental conditions of CO<sub>2</sub> discharges, and thus our approach is valid in the relevant range of  $T_{va}/T_g < 8$ .

### e. e-V excitation

e-V processes are the primary sources of vibrational excitation in plasmas. So far in this work, the only e-V processes considered have been vibrational excitation from CO<sub>2</sub>( $v = 0$ ) to CO<sub>2</sub>( $v = 1$ ) and de-excitation from CO<sub>2</sub>( $v = 1$ ) to CO<sub>2</sub>( $v = 0$ ). In fact, monoquantum

and multiquantum excitation and de-excitation reactions through collisions of electrons with other vibrational levels are also important to determine the vibrational temperatures of  $\text{CO}_2$ , and may be relevant for the shape of the VDF. Here, as we want to study only the VDF in the asymmetric stretching mode, we only consider transitions in that mode. As in the work of Kozák and Bogaerts<sup>30</sup>, e-V excitation is only considered for collisions between electrons and the lowest states of  $\text{CO}_2$ , with  $v \leq 5$ . Even though the excitation of multiple quanta may be relevant for the VDF, it is not the object of this work, and thus only monoquantum excitation and de-excitation processes are taken into account. When these processes are implemented in the STS model, the VDFs observed in Fig. 7 are obtained for  $P_{dep} = 2, 000; 5, 000; 10, 000$   $\text{W cm}^{-3}$ .

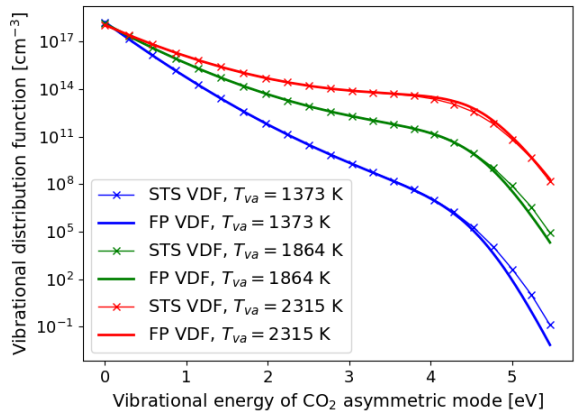


Figure 7: VDFs obtained with e-V, V-V<sub>n</sub>, V-V', V-T and V-V<sub>1</sub> processes, including dissociation, for  $P_{dep} = 2, 000; 5, 000$  and  $10, 000$   $\text{W cm}^{-3}$ . Results from STS and FP models.

By comparing the VDFs in Figs. 6 and 7, it can be noticed that  $T_{va}$  is increased with the inclusion of the e-V processes. For  $P_{dep} = 2, 000$   $\text{W cm}^{-3}$ ,  $T_{va} = 1373$  K, instead of 1333 without these e-V processes. For  $P_{dep} = 10, 000$   $\text{W cm}^{-3}$ ,  $T_{va} = 2315$  K, instead of 2146 without these e-V processes. The increase could be significantly higher with the inclusion of other e-V processes. The e-V reactions included only affect the lower levels of the VDF.  $T_{va}$  is changed but the bulk of the VDF still follows a Treanor at  $T_{va}$ . Thus, no change is necessary in the FP model to describe these processes. The FP VDFs presented in Fig. 7 have been obtained using the same parameters as those used for the VDFs in Fig. 6

and the same type of good agreement is obtained for  $T_{va} < 2500$  K. As can be observed, the inclusion of the monoquantum e-V processes for the 6 levels of lowest energy of the asymmetric stretching vibrational mode of CO<sub>2</sub> has not modified the tail of the VDFs and the agreement between the STS and FP calculations. It can not be discarded that the inclusion of other e-V processes would require a special treatment in the FP formulation, as performed in the works of Macheret, Rusanov and coworkers<sup>20,23</sup>.

## Conclusions

The use of the numerical Fokker-Planck (FP) approach to describe the vibrational kinetics of the asymmetric stretching vibrational mode of CO<sub>2</sub> has been validated in this work, through comparisons with a state-to-state (STS) model considering the same physical conditions and kinetic data. In particular, the detailed comparison of the vibrational distribution functions (VDFs) obtained in stationary conditions through the two approaches has been taken as criterium of validation. The validation has been carried out inside the theoretical limits of validity of the FP equation, that describes vibrational kinetics as drift and diffusion transport processes in the space of vibrational energy. As such, only monoquantum transitions have been considered. The validation has been performed at a gas temperature of 300 K and for a wide range of relevant vibrational temperatures, by describing one physical process at the time, thus validating the parameters used in the FP model to describe each process: V-V<sub>1</sub> exchanges, with and without dissociation; V-T relaxation; V-V' exchanges with the other vibrational modes of CO<sub>2</sub>; V-V<sub>n</sub> for vibrational temperatures below 2500 K; and e-V excitation of the lowest vibrational levels. Simultaneously, the effect of each of these crucial processes for the vibrational kinetics of polyatomic molecules has been evaluated, by assessing their influence on the STS calculation of vibrational temperature and on both the STS and FP VDFs.

The derivation of the FP equation exposed in this work provides the general theoretical

basis to apply this method to any system. However, the implementation of the kinetic scheme depicted in table 1 in the FP model has been shown to be not straightforward. In fact, the formulation of drift and diffusion coefficients has been shown to be dependent on the processes considered. Yet, the implementation of several processes shown in this work provides a basis for the application of the FP approach to more processes, molecules and physical conditions. In particular, we can foresee the interest to implement, for CO<sub>2</sub> or other molecules, multiquantum transitions, a more complete description of e-V reactions and intermode exchanges, vibrational exchanges between different molecules and further dissociation and recombination processes. The validity of multiquantum transitions in the FP model has to be tested, since these transitions may collide with the theoretical derivation of the FP equation. The inclusion of all other processes can be based on the formulations exposed in this work, but requires appropriate extensions and validation. The analytical works with the FP equation<sup>7,19,20</sup> can be particularly helpful for that aim. In future work we intend to deal with the implementation of these processes. Moreover, the validation procedure will be generalized for any gas temperature.

The FP model requires gas temperature, vibrational temperatures and number density of a few species as input parameters, which we have obtained from STS calculations. Once these parameters are known, the FP calculations of the stationary VDF are much faster, around three orders of magnitude faster, than the STS calculations. Thus, the use of the FP approach in multidimensional models is very promising for the prospect of modelling CO<sub>2</sub> plasma reactors taking into account vibrational non-equilibrium. However, the self-consistent use of the FP approach requires its coupling with calculations that provide the input parameters. The implementation of reduced STS models, considering only a few species, will be explored for this purpose, while avoiding the computational cost of full STS models that include dozens of species and hundreds or thousands of reactions. These steps will allow to use the FP approach self-consistently in physical conditions of CO<sub>2</sub> discharge experiments, such as those of plasma reactors for CO<sub>2</sub> conversion.

## Acknowledgements

The work presented in this paper is part of the European project KEROGREEN, which has received funding from the European Union's Horizon 2020 Research and Innovation Programme under Grant Agreement 763909. This work is also part of the Shell-NWO/FOM initiative 'Computational sciences for energy research' of Shell and Chemical Sciences, Earth and Life Sciences, Physical Sciences, FOM and STW. This work has also been carried out under TTW open technology project (grant nr. 15325) in collaboration with Gasunie, Stedin, DNVGL and Ampleon. The authors thank Prof. Annemie Bogaerts for sharing kinetic data. PV is grateful to Dr. Zdenek Bonaventura for helpful discussions on the state-to-state simulations.

## References

- (1) Goede, A.; van de Sanden, M. C. M. CO<sub>2</sub>-neutral fuels. *Europhys. News* **2016**, *47*, 22–26.
- (2) Guerra, V.; Silva, T.; Ogloblina, P.; Grofulov c, M.; Terraz, L.; da Silva, M. L.; Pintassilgo, C. D.; Alves, L. L.; Guaitella, O. The case for in situ resource utilisation for oxygen production on Mars by non-equilibrium plasmas. *Plasma Sources Sci. Technol.* **2017**, *26*, 11LT01.
- (3) Fridman, A. *Plasma chemistry*; Cambridge University Press, 2008.
- (4) Legasov, V. A.; Zhivotov, V. K.; Krashennnikov, E. G.; Krotov, M. F.; Patrushev, B. I.; Rusanov, V. D.; Rykunov, G. V.; Spektor, A. M.; Fridman, A. A.; Sholin, G. V. A nonequilibrium plasma-chemical process of CO<sub>2</sub> dissociation in high-frequency and ultra-high-frequency discharges. *Dokl. Akad. Nauk* **1978**, *238*, 66–69.
- (5) Moreno, S. H.; Stankiewicz, A. I.; Stefanidis, G. D. A two-step modelling approach

- for plasma reactors – experimental validation for CO<sub>2</sub> dissociation in surface wave microwave plasma. *React. Chem. Eng.* **2019**, *4*, 1253–1269.
- (6) Rusanov, V. D.; Fridman, A. A.; Sholin, G. V. CO<sub>2</sub> dissociation in a nonequilibrium plasma. *Zh. Tekh. Fiz.* **1979**, *49*, 2169–2175.
- (7) Capitelli, M. *Nonequilibrium vibrational kinetics*; Springer-Verlag, 1986.
- (8) Capitelli, M.; Colonna, G.; D’Ammando, G.; Pietanza, L. D. Self-consistent time dependent vibrational and free electron kinetics for CO<sub>2</sub> dissociation and ionization in cold plasmas. *Plasma Sources Sci. Technol.* **2017**, *26*, 055009.
- (9) Armenise, I.; Kustova, E. Mechanisms of coupled vibrational relaxation and dissociation in carbon dioxide. *J. Phys. Chem A* **2018**, *122*, 5107–5120.
- (10) Silva, T.; Grofulovic, M.; Klarenaar, B. L. M.; Morillo-Candas, A. S.; Guaitella, O.; Engeln, R.; Pintassilgo, C. D.; Guerra, V. Kinetic study of low-temperature CO<sub>2</sub> plasmas under non-equilibrium conditions. I. Relaxation of vibrational energy. *Plasma Sources Sci. Technol.* **2018**, *27*, 015019.
- (11) Peerenboom, K.; Parente, A.; Kozák, T.; Bogaerts, A.; Degrez, G. Dimension reduction of non-equilibrium plasma kinetic models using principal component analysis. *Plasma Sources Sci. Technol.* **2015**, *24*, 025004.
- (12) Berthelot, A.; Bogaerts, A. Modeling of plasma-based CO<sub>2</sub> conversion: lumping of the vibrational levels. *Plasma Sources Sci. Technol.* **2016**, *25*, 045022.
- (13) de la Fuente, J. F.; Moreno, S. H.; Stankiewicz, A. I.; Stefanidis, G. D. A new methodology for the reduction of vibrational kinetics in non-equilibrium microwave plasma: application to CO<sub>2</sub> dissociation. *React. Chem. Eng.* **2016**, *1*, 540–554.
- (14) Sahai, A.; Lopez, B.; Johnston, C. O.; Panesi, M. Adaptive coarse graining method for

- energy transfer and dissociation kinetics of polyatomic species. *J. Chem. Phys.* **2017**, *147*, 054107.
- (15) Kustova, E.; Mekhonoshina, M.; Kosareva, A. Relaxation processes in carbon dioxide. *Phys. Fluid* **2019**, *31*, 046104.
- (16) Koelman, P.; Yordanova, D.; Graef, W.; Mousavi, S. T.; van Dijk, J. Uncertainty analysis with a reduced set of input uncertainties selected using pathway analysis. *Plasma Sources Sci. Technol.* **2019**, *28*, 075009.
- (17) Brau, C. A. Classical theory of vibrational relaxation of anharmonic oscillators. *Physica* **1972**, *58*, 533–553.
- (18) Demura, A. V.; Macheret, S. O.; Rusanov, V. D.; Fridman, A. A.; Sholin, G. V. Diffusion theory of vibrational levels population of molecules in non-equilibrium plasma. *Proceedings of the 15<sup>th</sup> International Conference on Phenomena in Ionized Gases* **1981**, 55–56.
- (19) Fridman, A.; Kennedy, L. A. *Plasma physics and engineering*; CRC Press, Taylor and Francis Group, 2011.
- (20) Macheret, S. O.; Rusanov, V. D.; Fridman, A. A. Kinetics of the vibrations of molecules in a nonequilibrium plasma. *Sov. Phys. Dokl.* **1984**, *29*, 222–224.
- (21) Potapkin, B. V.; Rusanov, V. D.; Samarin, A. E.; Fridman, A. A.; Sholin, G. V. Dissociation of vibrationally excited CO<sub>2</sub> molecules in a plasma under conditions of equilibrium of the vibrational modes. *Khimiya Vysokikh Énergii* **1980**, *14*, 547–553.
- (22) Rusanov, V. D.; Fridman, A. A.; Sholin, G. V. Population of vibrationally excited states of diatomic molecules in a nonequilibrium plasma in the diffusion approximation. *Zh. Tekh. Fiz.* **1979**, *49*, 554–561.

- (23) Rusanov, V. D.; Fridman, A. A.; Sholin, G. V. The physics of a chemically active plasma with nonequilibrium vibrational excitation of molecules. *Sov. Phys. Usp.* **1981**, *24*, 447–474.
- (24) Diomede, P.; van de Sanden, M. C. M.; Longo, S. Insight into CO<sub>2</sub> dissociation in plasma from numerical solution of a vibrational diffusion equation. *J. Phys. Chem. C* **2017**, *121*, 19568–19576.
- (25) Diomede, P.; van de Sanden, M. C. M.; Longo, S. Vibrational kinetics in plasma as a functional problem: a flux-matching approach. *J. Phys. Chem. A* **2018**, *122*, 7918–7923.
- (26) Longo, S.; van de Sanden, M. C. M.; Diomede, P. Fokker-Planck equation for chemical reactions in plasmas. *Rendiconti Lincei. Scienze Fisiche e Naturali* **2019**, *30*, 25–30.
- (27) Lifshitz, E. M.; Pitaevskii, L. P. *Physical kinetics*; Pergamon press, 1979.
- (28) van Kampen, N. G. *Stochastic processes in physics and chemistry*; North-Holland Publishing Company, 1981.
- (29) Biberman, L. M.; Vorob'ev, V. S.; Yakubov, I. T. *Kinetics of nonequilibrium low-temperature plasmas*; Consultants Bureau, 1987.
- (30) Kozák, T.; Bogaerts, A. Splitting of CO<sub>2</sub> by vibrational excitation in non-equilibrium plasmas: a reaction kinetics model. *Plasma Sources Sci. Technol.* **2014**, *23*, 045004.
- (31) Armenise, I.; Kustova, E. Effect of asymmetric mode on CO<sub>2</sub> state-to-state vibrational-chemical kinetics. *J. Phys. Chem A* **2018**, *122*, 8709–8721.
- (32) Hagelaar, G. J. M.; Pitchford, L. C. Solving the Boltzmann equation to obtain electron transport coefficients and rate coefficients for fluid models. *Plasma Sources Sci. Technol.* **2005**, *14*, 722–733.
- (33) Pancheshnyi, S.; Biagi, S.; Bordage, M. C.; Hagelaar, G. J. M.; Morgan, W. L.; Phelps, A. V.; Pitchford, L. C. The LXCat project: electron scattering cross sections

and swarm parameters for low temperature plasma modeling. *Chem. Phys.* **2012**, *398*, 148–153.

- (34) Phelps, A. V. Phelps database. 2018; [www.lxcat.net](http://www.lxcat.net), retrieved on October 2018.
- (35) Hairer, E.; Wanner, G. *Solving ordinary differential equations II: Stiff and differential algebraic problems*; Springer-Verlag, 1996.
- (36) Unige, RADAU5 solver. [www.unige.ch/~hairer/software.html](http://www.unige.ch/~hairer/software.html).
- (37) Obrusník, A.; Bílek, P.; Hoder, T.; Simek, M.; Bonaventura, Z. Electric field determination in air plasmas from intensity ratio of nitrogen spectral bands: I. Sensitivity analysis and uncertainty quantification of dominant processes. *Plasma Sources Sci. Technol.* **2018**, *27*, 085013.
- (38) Simek, M.; Bonaventura, Z. Non-equilibrium kinetics of the ground and excited states in N<sub>2</sub>-O<sub>2</sub> under nanosecond discharge conditions: extended scheme and comparison with available experimental observations. *J. Phys. D: Appl. Phys.* **2018**, *51*, 504004.
- (39) Treanor, C. E.; Rich, J. W.; Rehm, R. G. Vibrational relaxation of anharmonic oscillators with exchange-dominated collisions. *J. Chem. Phys.* **1968**, *48*, 1798–1807.

## TOC Graphic

